Published in final edited form as:
Mol Cell Neurosci. 2008 October ; 39(2): 258–267. doi:10.1016/j.mcn.2008.07.004.

Assessment of functional recovery and axonal sprouting in oligodendrocyte-myelin glycoprotein (OMgp) null mice after spinal cord injury

Benxiu Ji[a,1], **Lauren C. Case**[b,1], **Kai Liu**[c], **Zhaohui Shao**[a], **Xinhua Lee**[a], **Zhongshu Yang**[a], **Joy Wang**[a], **Tim Tian**[a], **Svetlana Shulga-Morskaya**[a], **Martin Scott**[a], **Zhigang He**[c], **Jane K. Relton**[a], and **Sha Mi**[a,*]

[a]Department of Discovery Biology, Biogen Idec Inc., 14 Cambridge Center, Cambridge MA, 02142, USA

[b]Graduate Program in Neurosciences, Stanford University, Stanford, CA 94305, USA

[c]Division of Neuroscience, Children's Hospital, Harvard Medical School, Boston, MA 02115, USA

Abstract

Oligodendrocyte-myelin glycoprotein (OMgp) is a myelin component that has been shown *in vitro* to inhibit neurite outgrowth by binding to the Nogo-66 receptor (NgR1)/Lingo-1/Taj (TROY)/p75 receptor complex to activate the RhoA pathway. To investigate the effects of OMgp on axon regeneration *in vivo*, OMgp$^{-/-}$ mice on a mixed 129/Sv/C57BL/6 (129BL6) or a C57BL/6 (BL6) genetic background were tested in two spinal cord injury (SCI) models — a severe complete transection or a milder dorsal hemisection. OMgp$^{-/-}$ mice on the mixed 129BL6 genetic background showed greater functional improvement compared to OMgp$^{+/+}$ littermates, with increased numbers of cholera toxin B-labeled ascending sensory axons and 5-HT^{+} descending axons and less RhoA activation after spinal cord injury. Myelin isolated from OMgp$^{-/-}$ mice (129BL6) was significantly less inhibitory to neurite outgrowth than wild-type (wt) myelin *in vitro*. However, OMgp$^{-/-}$ mice on a BL/6 genetic background showed neither statistically significant functional recovery nor axonal sprouting following dorsal hemisection.

Keywords

Myelin; Axonal regeneration; Spinal cord injury; Nogo; MAG; OMgp

Introduction

Axonal regeneration in the adult spinal cord is thought to be at least partially blocked after injury by inhibitory myelin components (Filbin, 2003; Yiu and He, 2006), including Nogo (Chen et al., 2000; Grandpré et al., 2000), myelin-associated glycoprotein (MAG) (McKerracher et al., 1994; Mukhopadhyay et al., 1994) and oligodendrocyte-myelin glycoprotein (OMgp) (Wang et al., 2002a; Voure'h and Andres, 2004). These components share a common receptor complex, Nogo-66 (NgR1)/p75/Troy/LINGO-1 (Mi et al., 2004; Park et al., 2005; Shao et al., 2005; Wang et al., 2002b), which activates RhoA to block axonal

[1]Authors contributed equally to this work.

*Corresponding author. Fax: +1 617 679 3148. *E-mail address:* sha.mi@biogenidec.com (S. Mi).

regeneration (Dubreuil et al., 2003; Fournier et al., 2003; Mi et al., 2004). Inhibition of Nogo-66, MAG or OMgp using soluble NgR1 receptor ectodomain, soluble LINGO-1 or peptide inhibitor (NEP1-40) or RhoA inhibitors in models of spinal cord injury results in enhanced motor function recovery and axonal sprouting of some axonal tracts such as raphespinal and corticospinal tract (CST) fibers (Dubreuil et al., 2003, Li and Strittmatter, 2003; Li et al., 2004, 2005; Ji et al., 2005, 2006).

The individual contribution of myelin inhibitory proteins to inhibit axonal regeneration *in vivo* has been investigated in spinal cord injury models using genetically mutated mice. In the absence of MAG, mutant animals do not exhibit enhanced regeneration (Bartsch et al., 1995). Mutations in Nogo-A and Nogo-A/B/C have been reported to result in limited or no sprouting/regeneration of corticospinal axons (Kim et al., 2003; Simonen et al., 2003; Zheng et al., 2003). Mice deficient in NgR1 exhibit limited raphespinal and rubrospinal fiber regeneration but no CST regeneration (Kim et al., 2004; Zheng et al., 2005). These variable outcomes have been attributed in part to genetic background, age, severity of injury, and differential growth capacity of axon tracts (Dimou et al., 2006; Cafferty and Strittmatter, 2006). Deletion of p75NTR did not result in regeneration of either ascending or descending pathways in spinal cord (Song et al., 2004), however, the limited expression of this protein in spinal cord axons (Song et al., 2004) and the finding that Troy can substitute for p75 in the Nogo-66 receptor complex *in vitro* (Shao et al., 2005; Park et al., 2005) leaves open the question of a role for Troy or other TNF receptor members in regenerative processes.

The role of the myelin inhibitory component OMgp has heretofore remained unexplored *in vivo*. Here we demonstrate enhanced functional recovery, axon regeneration and less RhoA-GTP activation on a mixed 129/Sv/C57BL/6 (129BL6) genetic background OMgp$^{-/-}$ mice, but not on a C57BL/6 (BL6) genetic background OMgp$^{-/-}$ mice after spinal cord injury (SCI).

Results

Generation of OMgp$^{-/-}$ null mice

Fig. 1A illustrates the construct used to target the OMgp locus and to replace the entire exon encoding OMgp (Mikol et al., 1993) with eGFP and NEO genes immediately following the ATG start codon. The chimeric founder mice were backcrossed to BL6 strain for 2 generations to produce OMgp$^{-/-}$ mice and OMgp$^{+/+}$ littermates on a mixed 129BL6 background. Additional backcrosses were performed for more than 10 generations to produce OMgp$^{-/-}$ mice and OMgp$^{+/+}$ littermates on the BL6 background. The genotype of the OMgp locus was determined by PCR using tail DNA (data not shown). Loss of OMgp transcripts and protein expression in OMgp$^{-/-}$ brain and spinal cord tissues were confirmed by RT-PCR (Fig. 1B) and Western Blot analysis (Fig. 1C). OMgp$^{-/-}$ mice were viable and fertile and did not differ phenotypically from their heterozygote or wild-type littermates observed in the open-field test prior to experimental SCI.

Assessing functional recovery after SCI in OMgp$^{-/-}$ mice

To determine whether a lack of OMgp improves functional recovery after SCI, OMgp$^{-/-}$ and OMgp$^{+/+}$ mice were tested in two spinal cord injury models, and hindlimb locomotor function was assessed using the Basso Mouse Scale (BMS; Basso and Fisher, 2003; Basso et al., 2006) 1 day and 3 days after SCI and weekly thereafter for 6 weeks.

Complete transection of the spinal cord was first performed in the 129BL6 background mice. All mice received a score of 0 on day 1 after SCI, confirming the hindlimb paralysis associated with a complete lesion (Fig. 2A). To further confirm that all spinal cords had been completely transected in the mice, all cords were sectioned and immunostained for GFAP. No intact tissue

bridges were found between the two transected stumps in any of the injured animals (Fig. 2B). Two weeks after injury, OMgp$^{-/-}$ mice showed increased BMS scores compared to OMgp$^{+/+}$ mice with continuous improvement for 6 weeks. These BMS scores reached a statistically significant difference in the OMgp$^{-/-}$ mice from 4 weeks onwards (Fig. 2A). Because of the severe nature of the complete transection injury model, the BMS scores were low overall and no plantar stepping capability was observed in any mice from the OMgp$^{+/+}$ group. In contrast, some OMgp$^{-/-}$ mice demonstrated extensive ankle movements and some animals performed plantar placements or occasional dorsal-steps, whereas most OMgp$^{+/+}$ mice displayed slight ankle movement. This result suggests that blocking OMgp promotes functional recovery after SCI.

We next evaluated OMgp function using a milder injury paradigm in the129BL6 background mice. Following dorsal hemisection, locomotor function was assessed using the BMS rating system in combination with subscoring based on assessing fine locomotor functions including stepping capability, paw positioning, and trunk and tail stabilities (Basso et al., 2006). BMS scores in the OMgp$^{-/-}$ group were lower than the OMgp$^{+/+}$ group 1 day after dorsal hemisection (Table 1), suggesting the OMgp$^{-/-}$ group started out more severely injured than did the OMgp$^{+/+}$ group. Due to the functional impairments initially observed between the two groups, the BMS scores were normalized as BMS value change relative to day 1 score to achieve a better comparison of recovery rates between the two groups (personal communication with Michele Basso). Fig. 3A shows that change in BMS in OMgp$^{-/-}$ mice quickly increased over OMgp$^{+/+}$ mice 7 days after injury (P<0.05), indicating that the loss of OMgp may lead to a better recovery in the early functional improvement on the lower scale of the BMS after SCI. Seven through 42 days after injury, BMS scores for OMgp$^{-/-}$ mice remained higher compared to OMgp$^{+/+}$ mice despite the fact that recovery rates for the two groups were similar (Fig. 3A), indicating that OMgp has less impact on the late functional recovery on the high scale of the BMS. To further confirm this early functional recovery observed in the OMgp$^{-/-}$ group, we used another analysis of linear regressions to compare recovery rates between the two groups from day 1-7 post-injury. Linear regression demonstrated that the slope of recovery of the OMgp$^{-/-}$ group was 3-fold steeper than the OMgp$^{+/+}$ group in the first week (Supplemental Fig. 1A), demonstrating that a greater functional improvement occurred within the first week in the OMgp$^{-/-}$ group. A repeated ANOVA also confirmed statistically significant differences 3 and 7 days after injury (P<0.01, Supplemental Fig. 1B) between wt and OMgp$^{-/-}$ mice 1-7 days post-injury. Since the BMS subscore is better for discriminating the differences in the fine details of the locomotion that may not be differentiated by BMS (Basso et al., 2006), the subscore was used to determine whether OMgp is involved in late locomotor recovery when animals have attained frequent plantar stepping (BMS $\geq$ 5). Similar to the BMS, the initial impairments in locomotion were observed in both groups (Table 2), the normalized BMS subscores were expressed as change in BMS subscores. As Fig. 3B illustrates, the subscore value change in OMgp$^{-/-}$ group greatly increased over OMgp$^{+/+}$ group 1 week and onwards (P<0.05). Linear regression analysis demonstrated that the recovery rate was overall faster in the OMgp$^{-/-}$ group (slope=0.13, r^2=0.8) than in OMgp$^{+/+}$ group (slope=0.04, r^2=0.7) after injury (Supplemental Fig. 2A). Using linear regression analyzing from day 1-7 post-injury, the slope of OMgp$^{-/-}$ group (slope=0.44, $_r^2$=0.9) increased 4-fold over the OMgp$^{+/+}$ group (slope=0.11, $_r^2$=0.6) in the first week of recovery (Supplemental Fig. 2B). The slope of the OMgp$^{-/-}$ group (slope=0.08, $_r^2$=0.7) continued to rise and reached a 2-fold increase above the OMgp$^{+/+}$ group (slope=0.04, $_r^2$=0.6) from days 7 to 42 after SCI (Supplemental Fig. 2C), suggesting that OMgp may not only contribute to early functional recovery on the lower scale of the BMS but may also be involved in late detailed locomotor improvement as well.

To further confirm if loss of OMgp leads to functional recovery, we tested OMgp null and wild-type mice on a BL6 genetic background using a milder dorsal-hemisection model. OMgp$^{-/-}$ mice were again observed a slightly lower BMS scores than OMgp$^{+/+}$ mice 1 day

after SCI (Table 3). However, the normalized change in BMS and BMS subscores (data not shown) revealed no statistically significant in OMgp null mice (P>0.05, Fig. 3C).

Assessing axonal regeneration after SCI in OMgp$^{-/-}$ mice

To examine whether functional recovery is correlated with axonal regeneration after SCI in OMgp$^{-/-}$ mice on a 129BL6 background, we focused on examining the regeneration of several descending axon tracts including both corticospinal and serotonergic (5-HT^{+}) raphespinal systems, and ascending sensory tract after complete or partial transection of the spinal cord.

The descending serotonergic (5-HT^{+}) raphespinal system, which contributes to locomotor function in the spinal cord (Kim et al., 2004), was assessed by immunostaining for 5HT^{+} axons following a complete transection of the spinal cord. As expected, abundant 5HT^{+} axons were observed in the intermediolateral column around the central canal and in the ventral gray matter in transverse sections rostral to the lesion (Fig. 4A). In sagittal sections, most 5-HT^{+} axons in both experimental groups stopped at the proximal border of the lesion (Fig. 4B). Numerous outgrowths of 5HT^{+} axons were observed in the gray matter caudal to the lesion in OMgp$^{-/-}$ mice (Figs. 4C and D), suggesting enhanced sprouting of 5-HT^{+} fibers in OMgp$^{-/-}$ mice. Quantification of 5-HT^{+} axons revealed a 3-fold increase in 5HT^{+} axons in injured spinal cord 0-2.5 mm caudal to the lesion in OMgp$^{-/-}$ mice compared to OMgp$^{+/+}$ mice (Fig. 4E). Further from the lesion, (2.5-5 mm), 5-fold more 5HT^{+} axons were observed in OMgp$^{-/-}$ relative to OMgp$^{+/+}$ mice (Fig. 4E).

To assess axon regeneration in ascending sensory tracts, L5 DRG were injected with Cholera Toxin B conjugated with Alexa 488 6 weeks after complete transection of the spinal cord. All cords displayed strong and uniform labeling in the nerve root surrounding the injected dorsal root ganglion (DRG) 1 week after the tracer was injected (Fig. 5A). Sections were immunostained with an anti-Alexa 488 antibody to enhance visualization, thereby revealing retrogradely labeled motorneurons and afferent axons in the dorsal gray matter caudal to the lesion (Fig. 5B). While the retrogradely labeled axons in both groups mostly stopped at the distal border of the lesion (Fig. 5C), outgrowths of sensory axons were observed in the spinal cord below the lesion in OMgp$^{-/-}$ mice (Figs. 5C-E) and some labeled axons were seen in the gray matter rostral to the lesion (Fig. 5F), suggesting enhanced sensory fibers in OMgp$^{-/-}$ mice. To quantify axons that had grown beyond the lesion, ascending axons were counted 0-5 mm rostral to the injury in sagittal sections under the microscope. A 2-fold increase in the number of ascending axons was observed in OMgp$^{-/-}$ versus wild-type sections (Fig. 5G). Enhanced functional recovery in the OMgp$^{-/-}$ mice is therefore associated with improved axon regeneration. To examine the role of OMgp in CST axon regeneration and sprouting, mice underwent dorsal hemisection at T10 to disrupt the main CST in the dorsal column and the minor CST component in the dorsolateral funiculus. Six weeks after the injury, the CST axons were traced with BDA from sensorimotor cortex. The animals were then allowed to survive for another two weeks, and the regenerative and sprouting CST axons were examined at 5 mm caudal to the lesion. Fig. 6 illustrates that most CST axons were detected rostral to the lesion from both transverse (Fig. 6A) and sagittal sections (Fig. 6B). However, very few axons were observed caudal to the lesion from both wild-type and mutant mice (Fig. 6C). No statistical difference was seen between the wild-type and the mutant mice (P>0.05, Fig. 6C).

Rho inactivation after SCI in OMgp$^{-/-}$ mice

Since Rho activation by myelin inhibitors prevents axonal regeneration, and blocking Rho activation promotes regeneration after SCI (Dergham et al., 2002; Dubreuil et al., 2003; Yiu and He, 2006), we measured RhoA-GTP levels in spinal cord homogenates prepared from the transection injury site of both OMgp$^{-/-}$ and OMgp$^{+/+}$ mice on the 129BL6 background (Fig.

7A). A two-fold increase in RhoA-GTP levels was seen 3 days after SCI in $OMgp^{+/+}$ mice, while no significant change was observed in $OMgp^{-/-}$ mice (Fig. 7B).

Reduced inhibition of neurite outgrowth by myelin isolated from $OMgp^{-/-}$ mice

Myelin components are potent inhibitors of neurite outgrowth (Wang et al., 2002a), so the deletion of OMgp has the potential to lessen its inhibitory function. To test this hypothesis, myelin from $OMgp^{-/-}$ and wild-type mice on a 129BL6 background was isolated and assayed at various concentrations for neurite outgrowth inhibition using postnatal day 6 DRG neurons. Neurons were fixed and stained with anti-βIII tubulin antibody after 16 h in culture. Neurite length was significantly longer at 0.5 μg $OMgp^{-/-}$ myelin compared to wild-type myelin (Figs. 8A, B). At higher concentrations (1 or 2 μg) of $OMGP^{-/-}$ myelin, no difference in neurite length was observed in comparison to wild-type myelin (Figs. 8A, B). Increased inhibition of neurite outgrowth was observed when purified OMgp protein (1 μg/ml) was spiked into myelin isolated from $OMgp^{-/-}$ or wild-type mice (Figs. 8A, B). This suggests that, at low concentrations, OMgp null myelin is less growth-inhibitory, whereas at higher concentrations, other inhibitory myelin components (MAG, Sema4D and Nogo-A) may substitute for OMgp to inhibit neurite outgrowth.

Discussion

Our data demonstrate that deletion of the *OMgp* gene from mice improved functional recovery, especially early functional recovery, in two spinal cord injury models (complete transection and hemitransection) in OMgp null mice on a 129BL6 background. This may be in part explained by the enhanced $5\text{-}HT^{+}$ fiber sprouting observed after complete transection. Mechanistically, we observed reduced RhoA activation in the lesion site and reduced inhibitory activity of CNS myelin from $OMgp^{-/-}$ mice, providing *in vivo* support for the *in vitro* evidence that OMgp is an inhibitory molecule for axon regrowth after injury.

Our *in vivo* studies have been performed double blind as a collaboration among three different institutions. In the complete transection study, $OMgp^{-/-}$ mice exhibited statistically significant functional recovery on the lower BMS scale when compared to $OMgp^{+/+}$ mice 4 weeks after SCI. Similarly, in the milder SCI dorsal-hemisection study, $OMgp^{-/-}$ mice showed marked functional improvement on the higher BMS scale when compared to $OMgp^{+/+}$ mice 1 week after SCI. The $OMgp^{-/-}$ group had a more severe initial deficits than the $OMgp^{+/+}$ group (possibly due to the defect in the node of Ranvier as described by Huang et al., 2005). Nevertheless, the $OMgp^{-/-}$ mice quickly recovered function after injury and change from baseline BMS scores rose quickly and exceeded those of $OMgp^{+/+}$ mice 1 week after injury. Once most animals in both genotypes achieved a threshold (score of 5) of frequent plantar stepping 1 week after injury, $OMgp^{-/-}$ mice continued to show greater functional recovery in the fine detailed locomotion tests represented by change in BMS subscores. We also demonstrated a correlation between improved functional recovery with enhanced axonal regeneration after SCI in $OMgp^{-/-}$ mice. Western blot analysis showed that Nogo-A protein level, but not MAG (data not shown) and RhoA, dramatically increased in $OMgp^{+/+}$ mice and no changes were observed in $OMgp^{-/-}$ mice after injury (data not shown), suggesting that loss of OMgp may decrease the expression of other inhibitory myelin components and RhoA activation for promoting functional recovery and axon regeneration on a 129BL6 background after spinal cord injury.

In our studies, behavioral improvements and enhanced axonal regeneration were only demonstrated in the OMgp mutant mice from a mixed 129BL6 background. We did not see a statistically significant difference in functional recovery following dorsal hemisection between OMgp mutants and wild-type mice on the BL6 background. This strain-specific difference resulting in differences in axonal regeneration and functional recovery after SCI was also

reported by others (Dimou et al., 2006; Cafferty et al., 2007; Basso et al., 2006). More pronounced axonal regeneration *in vivo* and *in vitro* has been reported in 129/Sv strain than BL6 strain (Dimou et al., 2006). This may be explained by a reduced inflammatory/immune response to the injury via reduced microglia/macrophage activation (Ma et al., 2004; Dimou et al., 2006) and less neutrophil infiltration (Robson et al., 2003) into the lesion vicinity, altering cytokine production and reducing complement activation (Robson et al., 2003). Less chondroitin sulfate proteoglycans have also been reported in the 129/Sv strain than the BL6 strain (Dimou et al., 2006). The diminished early inflammatory response and scar formation could protect intact tissue from further damage via immune cell infiltration and lead to enhanced axonal regeneration resulting in functional recovery. It also may be partly due to lower endogenous myelin inhibitors like significantly lower Nogo-A protein expression in the 129/Sv strain compared to the BL6 strain (Dimou et al., 2006).

We observed that OMgp null mice had more severe injury at earlier stages after the SCI operation than did wild-type littermate controls although there are no differences in locomotion between the lines in uninjured animals. Recent studies describe that the anatomical distribution of OMgp is enriched at the node of Ranvier (Huang et al., 2005; Nie et al., 2006) and an abnormal node structure in the OMgp null mice. The abnormal node structure could be the cause of the severe injury after the initial injury operation.

In our study, we did not observe any CST axon regeneration after dorsal hemisection from either $OMgp^{-/-}$ mutants or $OMgp^{+/+}$ mice. It is possible that OMgp is not involved in CST regeneration or that it works together with other inhibitors to block *in vivo* regeneration blockade in this tract. Alternatively, this tract may be more sensitive to the severity of the lesion paradigm or to scar characteristics related to genetic background (Dimou et al., 2006; Cafferty and Strittmatter, 2006). Since only a few CST axons were detected below the lesion in both groups, it is also possible that the sensitivity of the current tract-tracing methodology may limit our ability to detect thin-diameter sprouts emanating from CST axons (Bareyre et al., 2005; Zhang et al., 2006).

In conclusion, loss of OMgp has been shown to promote functional recovery through axonal regeneration and reduction in RhoA activation in 129BL6 mice after spinal cord injury. This study furthers our understanding of how myelin inhibitors contribute to blockade of axonal regeneration in the central nervous system after spinal cord injury.

Experimental methods

OMgp targeting strategy and generation of null mice

To create an OMgp targeting construct, mouse genomic 129/Sv DNA was isolated from a lambda genomic library (Stratagene # 946313; Stratagene, LaJolla, CA); a 9.9 kb NotI-EcoRV fragment was subcloned into pBSK+, then targeted by homologous recombination in bacteria (Zhang et al., 2000) to insert a fusion reporter gene of eGFP and NEO at the initiating ATG. The final construct deleted the entire 1-1299 nt single exon of coding sequence of OMgp (Mikol et al., 1993) and was used to target the OMgp locus in V6.5 embryonic stem (ES) cells (obtained from R. Jaenisch) and injected into BL6 blastocysts to generate chimeric mice. Correctly targeted cells were identified by Southern blotting of XbaI-digested ES cell DNA. The chimeras were then backcrossed to BL6 strain mice resulting in a mixed background of 129BL6. The genotypes of wild-type, heterozygous and mutant mice were determined by three-primer PCR using tail DNA. The forward primer 5′-CCGAATGCTAACTGACCCATGC and the two reverse primers 5′-GAACAGTCCACATGCCTGTGCC and 5′-GATGCCCTTCAGCTCGATGCG yielded 207 bp wild-type and 496 bp mutant allele products in a 35-cycle reaction (94 °C for 20 s, 65 °C for 30 s, 72 °C for 30 s). Further genotype

confirmation was determined in mRNA and protein levels by RT-PCR and Western blot analysis from brain and spinal cord tissues.

Spinal cord injury

All experiments were performed in 8-week-old female mice. All procedures were performed in accordance with the NIH Guide for the Care and Use of Laboratory Animals and were approved by the Biogen Idec Institutional Animal Care and Use Committee.

Mice were anesthetized by injection with ketamine mixed with xylazine (90 mg ketamine/9.9 mg xylazine /kg, i.p.). The hair on the back was shaved and wiped with betadine and a 70% ethanol swab. A drape was used to cover the animal and a midline incision was made over the thoracic vertebrae. The paravertebral muscles were separated from the vertebral column and retracted, and a dorsal laminectomy was performed at T10. Surgeons were blinded to the mouse genotypes.

For the complete transection model, the vertebral column was stabilized using a pair of forceps, and a micro-scalpel was inserted into the midline of the spinal cord. The spinal cord was then cut from the dorsal to the ventral surface back and forth until clear separation was noted between the rostral and caudal stumps of the spinal cord (Inman and Steward, 2003; Spinal cord injury research techniques, Reeve-Irvine Research Center, UCI, 2003). A small piece of gelfoam was placed over the transected site.

For the dorsal-hemisection model, the spinal cord dura was punctured with a 30 gauge needle bilaterally to ensure a subsequent clean cut. Surgical micro-scissors were lowered to a depth of 0.8 mm and a cut lesion was made to the spinal cord. In order to further standardize the injury and to ensure that the dorsal components of the corticospinal tract were completely severed, a micro-scalpel was then inserted into the midline of the spinal cord at a depth of 0.8 mm below the dorsal surface and cut toward the lateral marker. The micro-scalpel cut was then repeated in the opposite direction. The paravertebral muscles were then closed with two sutures and the skin was closed with wound clips.

All procedures were performed under a surgical microscope. Animals were allowed to recover from anesthesia in a heating chamber. Buprenorphine (0.1 mg/kg, twice a day, sc) was administered for two days. Baytril (Enrofloxacin 2.5 mg/kg, twice a day, sc) was administered for 14 days. The initial doses of Buprenorphine and Baytril were administered pre-operatively. Bladders were expressed twice a day until bladder function returned.

Behavioral analysis

After spinal cord transection, animals were scored using the openfield BMS scoring system which is a 9-point scale designed specifically for evaluating locomotor function in mice. This measurement enables assessment of hindlimb function ranging from complete paralysis to normal locomotion (Basso and Fisher, 2003). Mice that had undergone a dorsal-hemisection lesion were also scored using the BMS subscoring system which is a 15-point scale designed for measuring more detailed fine locomotion ranging from frequent plantar steps to normal posture and tail stability at high levels of locomotor recovery (Basso et al., 2006). Each mouse was assessed for 4 min in the open field by two examiners blinded to the mouse genotypes. Average scores were calculated when left and right legs were different. The lower score was adopted if a discrepancy occurred between the two examiners. BMS scores and subscores were assessed on days1 and 3 after injury and weekly thereafter for 6 weeks. For the dorsalhemisection lesion paradigm, BMS and subscore results were expressed as a change from baseline for each animal.

Axon labeling

For axonal retrograde labeling of ascending sensory axons, six weeks after a complete transection of the spinal cord, mice were anesthetized as described above. The L5 nerve root near the DRG was exposed and 2 μl of 1% Cholera Toxin B conjugated with Alexa 488 (Molecular Probes) was slowly injected by using a 10-μl Hamilton microsyringe fitted with a glass micropipette (Inman and Steward, 2003; Spinal cord injury research techniques, Reeve-Irvine Research Center, UCI, 2003). After the injection was completed, the muscles overlying the nerve root were sutured with 5-0 silk and the skin was closed with wound clips.

For axonal anterograde labeling of CST, six weeks after dorsal hemisection of the spinal cord, mice were anesthetized as described above and a mixture of 10% rhodamine- and biotin-conjugated dextran amine (10,000 MW, Molecular Probes) in PBS was injected into the sensorimotor cortex using a glass micropipette fitted to a nanoliter injector (World Precision Instruments) in conjunction with an infusion pump (World Precision Instruments). The infusion rate of the tracer was 5 nl/s Three injection sites (0.4 μl each) were made 1.0 mm lateral to the midline, 0.5 mm anterior, 0.5 mm posterior, and 1.0 mm posterior to bregma, at a depth of 0.6 mm from the cortical surface (Zhang et al., 2003; Inman and Steward, 2003). At each location, the needle was left in position for additional 1 min before withdrawal. After the injections were completed, the skin overlying the skull was closed with wound clips.

Immunohistochemistry

Seven weeks after complete transection of the spinal cord or 8 weeks after dorsal hemisection of the spinal cord, animals were anesthetized with a lethal dose of ketamine/xylazine and perfused trans-cardially with heparin (10 iu/ml) in saline followed by 4% PFA in PBS. Spinal cords were removed and post-fixed in PFA overnight then cryopreserved in 30% sucrose overnight. The spinal cords were cut into 3 segments: 1) a segment of spinal cord containing 5 mm above to 5 mm below the lesion. This segment, containing the lesion, was sectioned into sagittal sections for evaluation of axons. 2) A segment of the spinal cord rostral to 1) above. This segment was cut into transverse sections. 3) A segment of the spinal cord caudal to 1) above. This segment was cut into transverse sections. Three tissue segments were embedded in OCT in one block, and cut into 20 μm sections. Every section was collected serially and mounted on gelatin-coated slides for histological analysis.

Primary antibodies used for immunofluorescent staining were rabbit polyclonal antibodies to Alexa 488 (1:2000, Molecular Probes) and Serotonin (5-HT) (1:10,000, Sigma). Rabbit polyclonal antibody to βIII tubulin (TUJ1, 1:500; Covance) was used to detect neurons in neurite outgrowth assay. The secondary antibody conjugated to either Alexa 594 or Alexa 488 was obtained from Molecular Probes (1:800).

Frozen tissue sections were permeabilized with 0.3% Triton X-100 (Sigma) in PBS, and blocked for 1 h at room temperature in a blocking solution consisting of PBS, 3% normal goat serum, 3% BSA and 0.3% Triton X-100. Primary antibodies were incubated overnight in a humidifying chamber at 4 °C. After washing 3 times with PBS plus 0.3% Triton X-100,tissue sections were incubated with corresponding secondary antibodies for 1 h at room temperature. Sections were then washed with PBS plus 0.3% Triton X-100 twice, washed once with PBS and mounted in Prolong Antifade Kit (Molecular Probes) and examined using a Leica fluorescent microscope.

Axonal quantification

Ascending sensory axons traced by Cholera Toxin B conjugated with Alexa 488 were visualized by immunostaining with anti-Alexa 488 antibody. All axons ≥100 μm in length were

included in the counts on sagittal sections 0-5 mm rostral to the lesion. Four to five sections, 180 μm apart, from each animal were examined using a Leica DM microscope.

Immuno-labeled 5-HT^+ axons were counted on sagittal sections 0-2.5 and 2.5-5 mm caudal to the lesion. Four to five sections, 180 μM apart, from each animal were analyzed using a Leica DM microscope. BDA-labeled CST axons were examined 5 mm caudal to the lesion on every sagittal section for every animal.

RhoA assay and Western blot

All mice were subjected to a complete transection of the spinal cord. Three days after injury, animals were sacrificed by CO_2inhalation. A 1 cm segment of spinal cord centered around the lesion site was harvested. Injured and uninjured spinal cords were homogenized and lysed in 50 mM Tris-HCl, pH 7.5, 1% Triton X-100, 0.5% sodium deoxycholate, 0.1% SDS, 500 mM NaCl, 10 mM $MgCl_2$, plus protease inhibitors, and processed as described previously (Ren et al., 1999). GTP-bound and total RhoA proteins were detected by Western blotting using an anti-RhoA mAb (Santa Cruz).

Neurite outgrowth assay

Primary dorsal root ganglion (DRG) neurons were prepared as described previously (Mi et al., 2004, Shao et al., 2005). Briefly, eight well chamber slides (Labtek, Rochester, NY) were coated with 0.1 mg/ml poly-D-lysine (Sigma) before spotting with 3 μl of 0 μg, 0.5 μg, 1 μg or 2 μg myelin extract from either wild-type or OMgp knockout mice with or without 1 μg/ml of AP-OMgp for 2 h at 37 °C. The slides were then coated with 10 μg/ml laminin (Invitrogen) for 1 h at 37 °C. DRG neurons (5000 cells/well) from P6 rats were dissociated, seeded onto the slides, and incubated at 37 °C in 5% CO_2 for 16 h. The slides were fixed in 4% paraformaldehyde/20% sucrose/PBS and immunostained with anti-βIII tubulin antibody. Neurite length was quantified by measuring the lengths of individual neurites (200 to 400 neurons per treatment condition) using OpenLab software (Improvision).

Statistical analysis

Two-way repeated measures analysis of variance (ANOVA) and Tukey post hoc analysis were used for BMS and subscore analyses. Unpaired Student's *t*-test was used to compare the two groups. One-way ANOVA and Tukey post hoc analysis were used to compare multiple groups for the neurite outgrowth analyses. Linear regression was analyzed by SAS to compare slopes between two groups assessing the rate of functional recovery.

Supplementary Material

Refer to Web version on PubMed Central for supplementary material.

Acknowledgments

We thank Michele Basso for helpful discussion on the behavioral analysis of BMS and BMS subscore systems. We thank Yongchen Wang for the helpful discussion on statistical analysis.

References

Bareyre FM, Kerschensteiner M, Misgeld T, Sanes JR. Transgenic labeling of the corticospinal tract for monitoring axonal responses to spinal cord injury. Nat. Med 2005;11:1355–1360. [PubMed: 16286922]

Bartsch U, Bandtlow CE, Schnell L, Bartsch S, Spillmann AA, Rubin BP, Hillenbrand R, Montag D, Schwab ME, Schachner M. Lack of evidence that myelin-associated glycoprotein is a major inhibitor of axonal regeneration in the CNS. Neuron 1995;15:1375–1381. [PubMed: 8845160]

Basso DM, Fisher LC. The Basso mouse scale for locomotion (BMS) is a more sensitive indicator of recovery than the BBB scale in mice with spinal cord injury. J. Rehab. Res. Dev 2003;40(S3):12.

Basso DM, Fisher LC, Anderson AJ, Jakeman LB, McTigue DM, Popovich PG. Basso mouse scale for locomotion detects differences in recovery after spinal cord injury in five common mouse strains. J. Neurotrauma 2006;23:635–659. [PubMed: 16689667]

Cafferty WB, Strittmatter SM. The Nogo-Nogo receptor pathway limits a spectrum of adult CNS axonal growth. J. Neurosci 2006;26:12242–12250. [PubMed: 17122049]

Cafferty WB, Kim JE, Lee JK, Strittmatter SM. Response to correspondence: Kim et al., “axon regeneration in young adult mice lacking Nogo-A/B.”. Neuron 2007;38:187–199.

Chen MS, Huber AB, van der Haar ME, Frank M, Schnell L, Spillmann AA, Christ F, Schwab ME. Nogo-A is a myelin-associated neurite outgrowth inhibitor and an antigen for monoclonal antibody IN-1. Nature 2000;403:434–439. [PubMed: 10667796]

Dergham P, Ellezam B, Essagian C, Avedissian H, Lubell WD, McKerracher L. Rho signaling pathway targeted to promote spinal cord repair. J. Neurosci 2002;22:6570–6577. [PubMed: 12151536]

Dimou L, Montani L, Duncan C, Simonen M, Schneider R, Liebscher T, Gullo M, Schwab ME. Nogo-A-deficient mice reveal strain-dependent differences in axonal regeneration. J. Neurosci 2006;26:5591–5693. [PubMed: 16723516]

Dubreuil CI, Winton MJ, McKerracher L. Rho activation patterns after spinal cord injury and the role of activated Rho in apoptosis in the central nervous system. J. Cell. Biol 2003;162:233–243. [PubMed: 12860969]

Filbin MT. Myelin-associated inhibitors of axonal regeneration in the adult mammalian CNS. Nat. Rev., Neurosci 2003;4:703–713. [PubMed: 12951563]

Fournier AE, Takizawa BT, Strittmatter SM. Rho kinase inhibition enhances axonal regeneration in the injured CNS. J. Neurosci 2003;23:1416–1423. [PubMed: 12598630]

Grandpré T, Nakamura F, Vartanian T, Strittmatter SM. Identification of the Nogo inhibitor of axon regeneration as a Reticulon protein. Nature 2000;403:439–444. [PubMed: 10667797]

Huang JK, Phillips GR, Roth AD, Pedraza L, Shan W, Belkaid W, Mi S, Fex-Svenningsen A, Florens L, Yates JR, Colman DR. Glial membranes at the node of Ranvier prevent neurite outgrowth. Science 2005;310:1813–1817. [PubMed: 16293723]

Inman DM, Steward O. Ascending sensory, but not other long-tract axons, regenerate into the connective tissue matrix that forms at the site of a spinal cord injury in mice. J. Comp. Neurol 2003;462:431–449. [PubMed: 12811811]

Ji B, Li M, Budel S, Pepinsky RB, Walus L, Engber TM, Strittmatter SM, Relton J. Effect of combined treatment with methylprednisolone and soluble Nogo-66 receptor after rat spinal cord injury. Eur. J. Neurosci 2005;22:587–594. [PubMed: 16101740]

Ji B, Wu WT, Yick LW, Lee X, Shao Z, Li M, Wang J, So K-F, McCoy JM, Pepinsky RB, Mi S, Relton J. LINGO-1 antagonist promotes functional recovery and axonal sprouting after spinal cord injury. Mol. Cell. Neurosci 2006;33:311–320. [PubMed: 17011208]

Kim JE, Li S, GrandPre T, Qiu D, Strittmatter SM. Axon regeneration in young adult mice lacking Nogo-A/B. Neuron 2003;38:187–199. [PubMed: 12718854]

Kim JE, Liu BP, Park JH, Strittmatter SM. Nogo-66 receptor prevents raphespinal and rubrospinal axon regeneration and limits functional recovery from spinal cord injury. Neuron 2004;44:439–451. [PubMed: 15504325]

Li S, Strittmatter SM. Delayed systemic Nogo-66 receptor antagonist promotes recovery from spinal cord injury. J. Neurosci 2003;23:4219–4227. [PubMed: 12764110]

Li S, Liu BP, Budel S, Li M, Ji B, Walus L, Li W, Jirik A, Rabacchi S, Choi E, et al. Blockade of Nogo-66, myelin-associated glycoprotein, and oligodendrocyte myelin glycoprotein by soluble Nogo-66 receptor promotes axonal sprouting and recovery after spinal injury. J. Neurosci 2004;24:10511–10520. [PubMed: 15548666]

Li S, Kim JE, Budel S, Hampton TG, Strittmatter SM. Transgenic inhibition of Nogo-66 receptor function allows axonal sprouting and improved locomotion after spinal injury. Mol. Cell. Neurosci 2005;29:26–39. [PubMed: 15866044]

Ma M, Wei P, Wei T, Ransohoff R, Jakeman LB. Enhanced axonal growth into a spinal cord contusion injury site in a strain of mouse (129x1/SvJ) with a diminished inflammatory response. J. Comp. Neurol 2004;474:469–486. [PubMed: 15174067]

McKerracher L, David S, Jackson DL, Kottis V, Dunn RJ, Braun PE. Identification of myelin-associated glycoprotein as a major myelin-derived inhibitor of neurite growth. Neuron 1994;13:805–811. [PubMed: 7524558]

Mi S, Lee X, Shao Z, Thill G, Ji B, Relton J, Levesque M, Allaire N, Perrin S, Sands B, et al. LINGO-1 is a component of the Nogo-66 receptor/p75 signaling complex. Nat. Neurosci 2004;7:221–228. [PubMed: 14966521]

Mikol DD, Rongnoparut P, Allwardt BA, Marton LS, Stefansson K. The oligodendrocyte-myelin glycoprotein of mouse: primary structure and gene structure. Genomics 1993;17:604–610. [PubMed: 8244377]

Mukhopadhyay G, Doherty P, Walsh FS, Crocker PR, Filbin MT. Anovel role for myelin-associated glycoprotein as an inhibitor of axonal regeneration. Neuron 1994;13:757–767. [PubMed: 7522484]

Nie D, MA Q, et al. Oligodendrocytes regulate formation of nodes of Ranvier via the recognition molecule OMgp. Neuron Glia Biol 2006;2:151–164. [PubMed: 17364021]

Park JB, Yiu G, Kaneko S, Wang J, Chang J, He XL, Garcia KC, He Z. A TNF receptor family member, TROY, is a coreceptor with Nogo receptor in mediating the inhibitory activity of myelin inhibitors. Neuron 2005;45:345–351. [PubMed: 15694321]

Ren XD, Kiosses WB, Schwartz MA. Regulation of the small GTP-binding protein Rho by cell adhesion and the cytoskeleton. Embo J 1999;18:578–585. [PubMed: 9927417]

Robson MG, Cook HT, Pusey CD, Walport MJ, Davies KA. Antibody-mediated glomerulonephritis in mice: the role of endotoxin complement and genetic background. Clin. Exp. Immunol 2003;133:326–333. [PubMed: 12930357]

Shao Z, Browning JL, Lee X, Scott ML, Shulga-Morskaya S, Allaire N, Thill G, Levesque M, Sah D, McCoy JM, et al. TAJ/TROY, an orphan TNF receptor family member, binds Nogo-66 receptor 1 and regulates axonal regeneration. Neuron 2005;45:353–359. [PubMed: 15694322]

Simonen M, Pedersen V, Weinmann O, Schnell L, Buss A, Ledermann B, Christ F, Sansig G, van der Putten H, Schwab ME. Systemic deletion of the myelin-associated outgrowth inhibitor Nogo-A improves regenerative and plastic responses after spinal cord injury. Neuron 2003;38:201–211. [PubMed: 12718855]

Song XY, Zhong JH, Wang X, Zhou XF. Suppression of p75NTR does not promote regeneration of injured spinal cord in mice. J. Neurosci 2004;24:542–546. [PubMed: 14724254]

Voure'h P, Andres C. Oligodendrocyte myelin glycoprotein (OMgp): evolution, structure and function. Brain Res. Brain Res. Rev 2004;45:115–124. [PubMed: 15145622]

Wang KC, Kim JA, Sivasankaran R, Segal R, He Z. P75 interacts with the Nogo receptor as a co-receptor for Nogo, MAG and OMgp. Nature 2002a;420:74–78. [PubMed: 12422217]

Wang KC, Koprivica V, Kim JA, Sivasankaran R, Guo Y, Neve RL, He Z. Oligodendrocyte-myelin glycoprotein is a Nogo receptor ligand that inhibits neurite outgrowth. Nature 2002b;417:941–944. [PubMed: 12068310]

Yiu G, He Z. Glial inhibition of CNS axon regeneration. Nat. Neurosci 2006;7:617–627.

Zhang Y, Muyrers JP, Testa G, Stewart AF. DNA cloning by homologous recombination in Escherichia coli. Nat. Biotechnol 2000;18:1314–1317. [PubMed: 11101815]

Zhang B, Lee K, Xie F. Genetic mouse models for studying inhibitors of spinal axon regeneration. Trends Neurosci 2006;29:640–646. [PubMed: 17030430]

Zheng B, Ho C, Li S, Keirstead H, Steward O, Tessier-Lavigne M. Lack of enhanced spinal regeneration in Nogo-deficient mice. Neuron 2003;38:213–224. [PubMed: 12718856]

Zheng B, Atwal J, Ho C, Case L, He XL, Garcia KC, Steward O, Tessier-Lavigne M. Genetic deletion of the Nogo receptor does not reduce neurite inhibition in vitro or promote corticospinal tract regeneration in vivo. Proc. Natl. Acad. Sci. U. S. A 2005;102:1205–1210. [PubMed: 15647357]

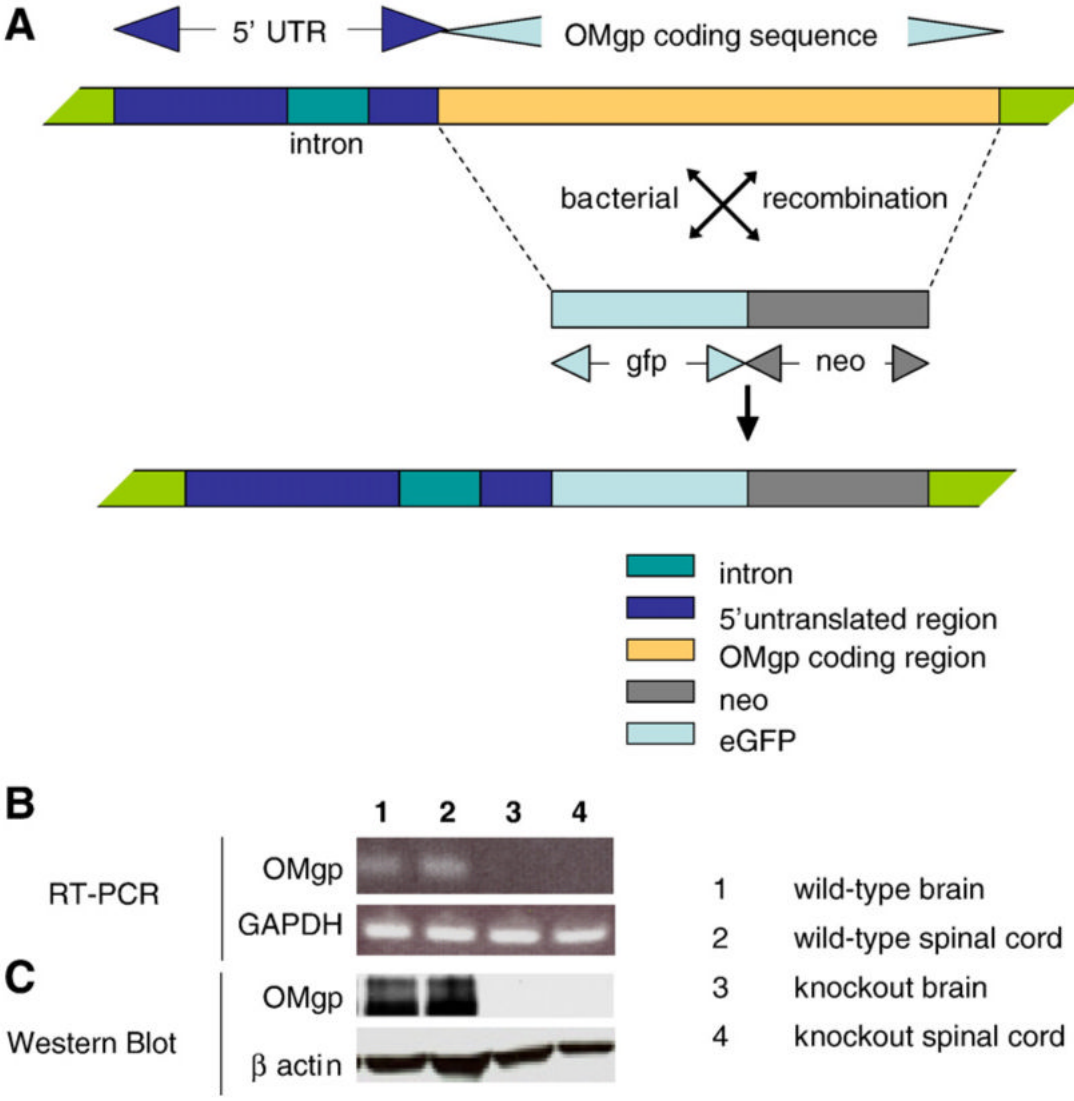

Fig. 1.

Deletion of the *OMgp* gene to create OMgp$^{-/-}$ mice. (A) Targeting strategy for deletion of the *OMgp* gene and replacement with eGFP and NEO genes after the starting code ATG. (B) mRNA expression levels from OMgp$^{+/+}$ brain (lane 1), OMgp$^{+/+}$ spinal cord (lane 2), OMgp$^{-/-}$ brain (lane 3) and OMgp$^{-/-}$ spinal cord tissues (lane 4) dissected from 8-week-old mice. (C) Western blot analysis of OMgp protein levels from spinal cord homogenates from 3 OMgp$^{+/+}$ and 3 OMgp$^{-/-}$ mice. Two bands of OMgp protein were present in wild-type mice, a membrane-bound version ~120 kDa as well as a soluble form of OMgp ~100 kDa.

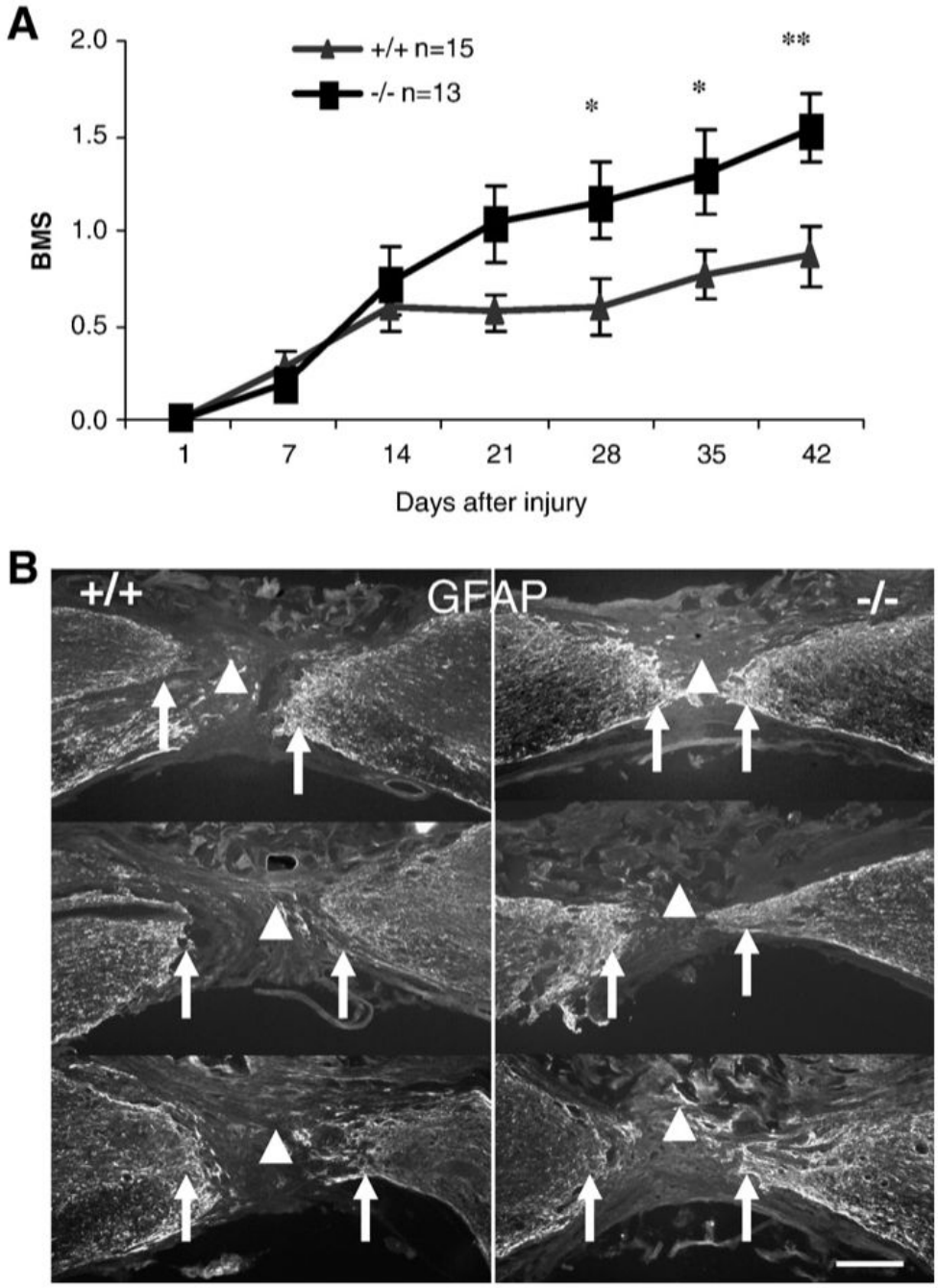

Fig. 2.

Assessment of functional recovery in OMgp$^{-/-}$ mice after complete transection of the spinal cord. (A) Evaluation of open-field locomotor function in OMgp$^{+/+}$ (n=15) and OMgp$^{-/-}$ (n=13) mice. All data are represented as mean±SEM, * = P<0.05, ** = P<0.01, two-way repeated measures ANOVA. (B) GFAP immunofluorescence staining of sagittal spinal cord sections from injured animals verified complete separation (arrowhead) between rostral and caudal stumps (arrows). Rostral is to the left and dorsal is up in all the sections. Each section depicts an individual animal. Scale bar, 150 μm.

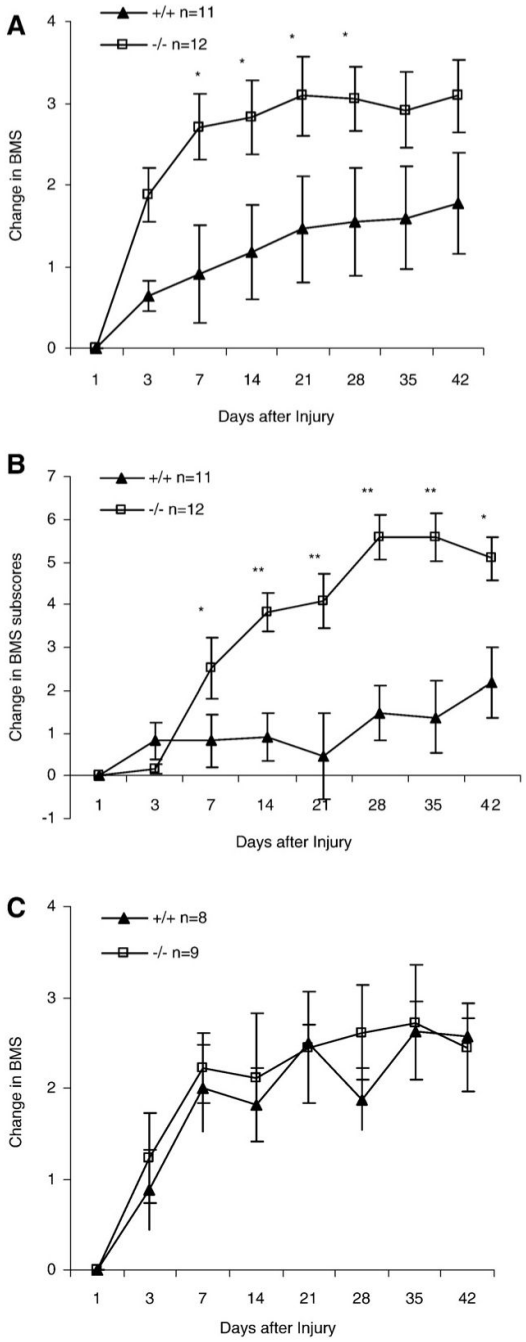

Fig. 3.

Assessment of functional recovery after dorsal-hemisection spinal cord lesion in $OMgp^{-/-}$ mice. Changes in (A) BMS score and (B) BMS subscore in $OMgp^{+/+}$ (n=11) and $OMgp^{-/-}$ (n=12) mice on a mixed 129BL6 background. (C) Changes in BMS score in $OMgp^{+/+}$ (n=8) and $OMgp^{-/-}$ (n=9) mice on BL6 background. All data are represented as mean±SEM, * = P<0.05, ** = P<0.01, two-way repeated measures ANOVA.

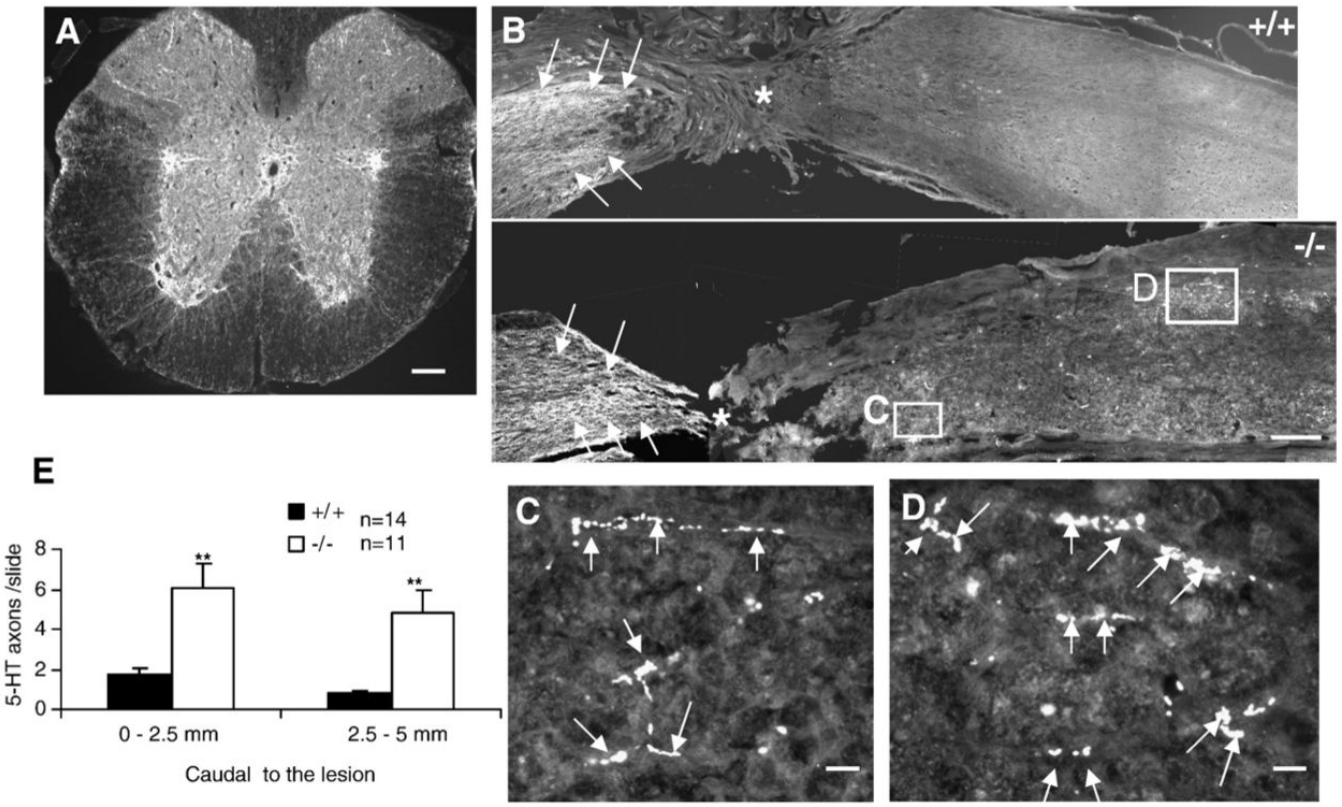

Fig. 4.

Descending 5-HT^{+} axon regeneration caudal to lesion in OMgp$^{-/-}$ mice 7 weeks after complete transection lesion. (A) Transverse-section view of 5-HT^{+} immunostained axons rostral to the lesion. Scale bar 120 μm. (B) 5-HT^{+} immunostained axons (arrows) in sagittal sections from OMgp$^{+/+}$ and OMgp$^{-/-}$ mice 7 weeks after complete transection. Rostral is to the left, caudal is to the right of the lesion (asterisk) and dorsal is up. Scale bar, 150 μm. (C and D) Higher magnification of 5-HT^{+} axons (arrows) from boxes in (B) of OMgp$^{-/-}$ mice. Scale bar, 15 μm. (E) The average number of 5-HT^{+} axons per sagittal section was quantified 0-2.5 mm and 2.5-5.0 mm caudal to the lesion in OMgp$^{+/+}$ (n=14) and OMgp$^{-/-}$ (n=11) mice. Data are presented as mean±SEM. ** $P \leq 0.01$, unpaired Student's t-test.

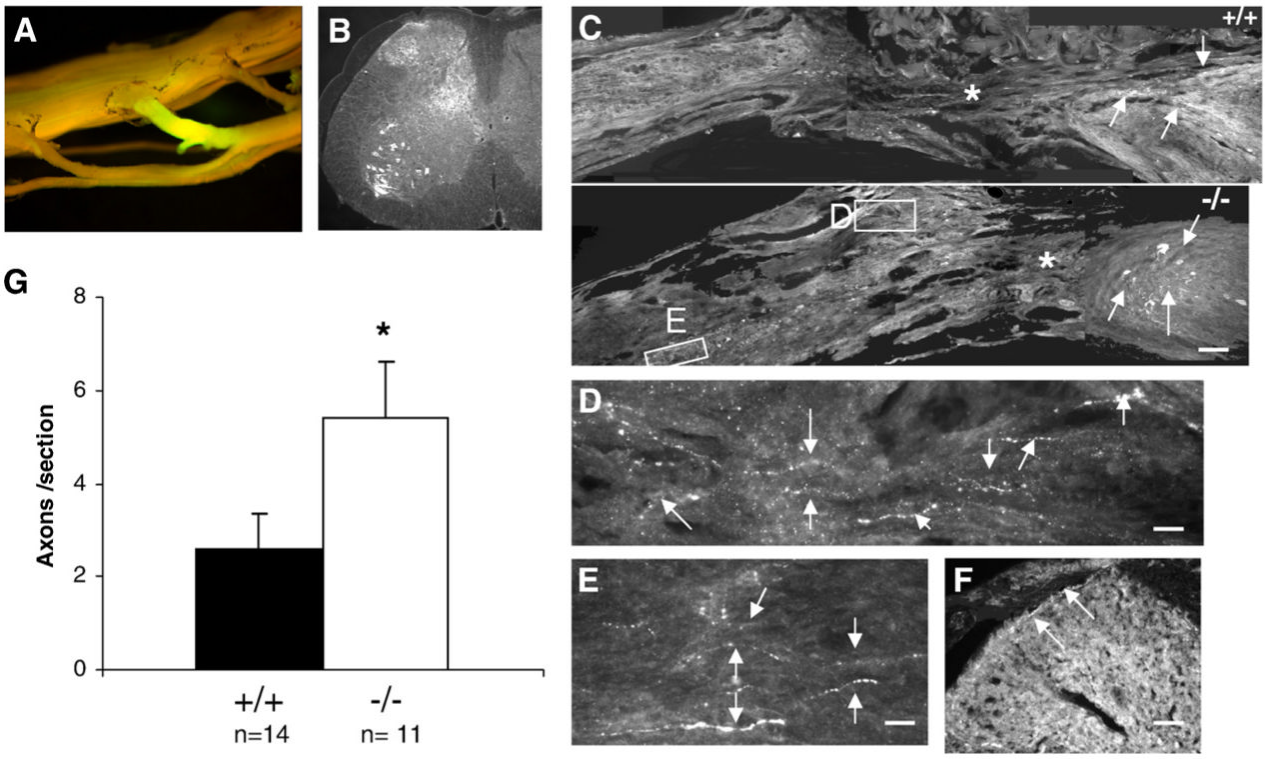

Fig. 5.

Axonal regeneration from ascending fibers of the spinal cord in OMgp$^{-/-}$ mice 7 weeks after complete transection lesion. (A) Fluorescent visualization of retrograde-labeled with Cholera Toxin B conjugated with Alexa 488 in the spinal cord, and in the L5 nerve root around DRG 1 week after injection. (B) Anti-Alexa 488 immunostaining for retrogradely labeled axons in a transverse section of the lumbar region of spinal cord. (C) Retrogradely labeled axons (arrows) stained with anti-Alexa 488 in sagittal sections from OMgp$^{+/+}$ and OMgp$^{-/-}$ mice 7 weeks after SCI. Rostral is to the left, caudal is to the right of the lesion (asterisk) and dorsal is up. Scale bar, 100 μm. (D and E) Higher magnification of axons (arrows) from boxes in (C) of OMgp$^{-/-}$ mice. CTB^{+} axons are located in the spinal cord, rostral to the lesion. Scale bar, 15 μm. (F) Cross-sectional view of axons (arrows) in dorsal GM 5 mm rostral to the lesion. Scale bar, 25 μm. (G) The average number of retrogradely labeled axons per sagittal section counted from 0-5 mm rostral to the lesion in OMgp$^{+/+}$ (n=14) and OMgp$^{-/-}$ (n=11) mice. All data are represented as mean±SEM. * P<0.05, unpaired Student's t-test.

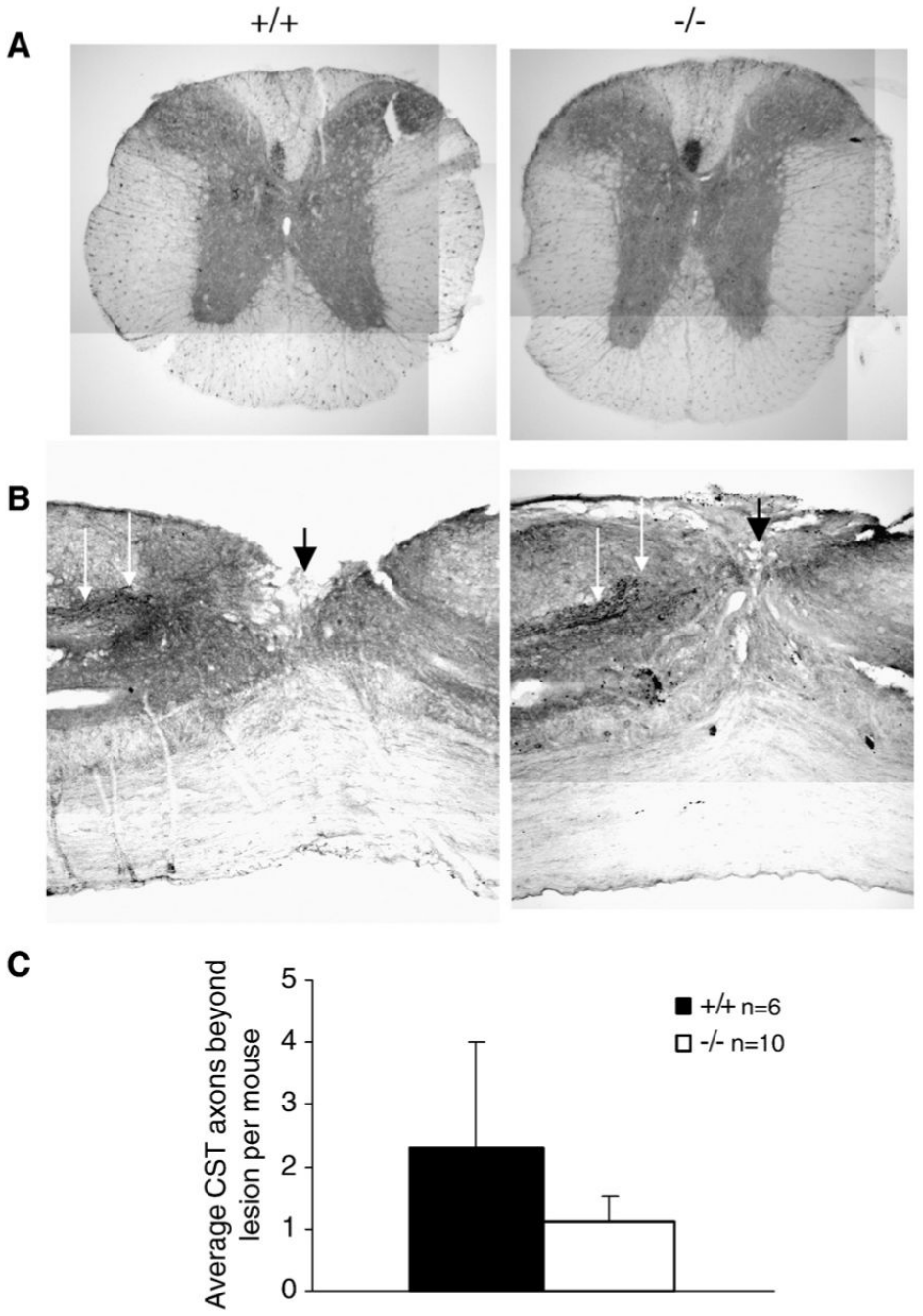

Fig. 6.

No detectable CST axon regeneration or sprouting after SCI in OMgp$^{-/-}$ mice. (A) Transverse- and (B) sagittal-section view of BDA-labeled CST axons (white arrows) rostral to the lesion from wild-type and OMgp mutant mice, verifying labeling technique. The injury site (black arrow) indicated that after a dorsal-hemisection lesion both the main CST and the minor dorsolateral CST component were completely disrupted. (C) Average number of axons per animal in OMgp$^{+/+}$ (n=6) and OMgp$^{-/-}$ (n=10) mice that traversed the lesion. Data are presented as mean±SEM.

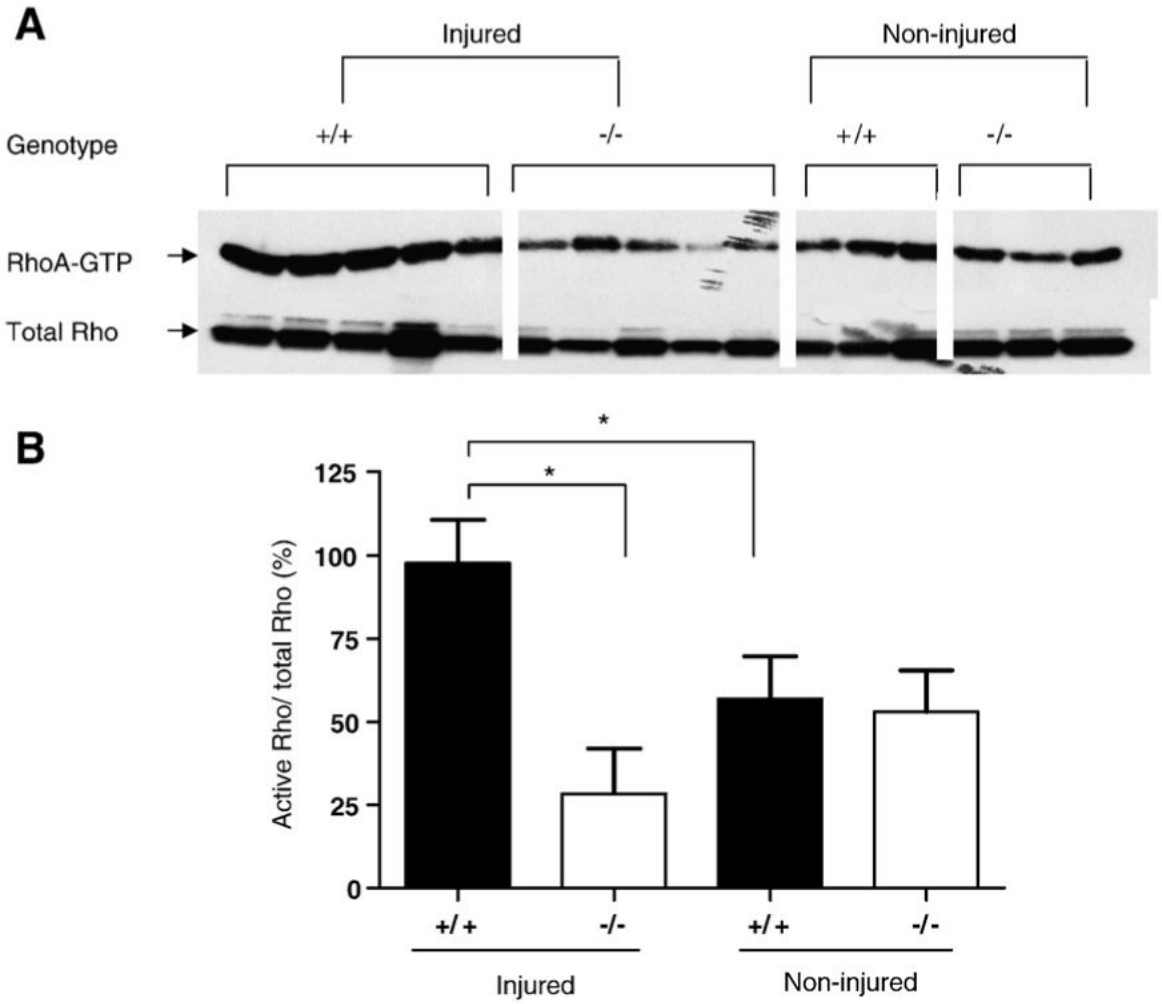

Fig. 7.

Lack of RhoA activation after SCI in OMgp$^{-/-}$ mice. (A) Active GTP-bound RhoA (RhoA-GTP) in spinal cord homogenates of OMgp$^{+/+}$ and OMgp$^{-/-}$ mice before and after SCI by pull-down assay. RhoA-GTP and total RhoA detected by Western blotting to anti-RhoA monoclonal antibody. (B) Quantification of relative RhoA-GTP density percentage of OMgp$^{+/+}$ and OMgp$^{-/-}$ mice before and after SCI. Data are presented as mean±SEM. * = P<0.05, unpaired Student's *t*-test.

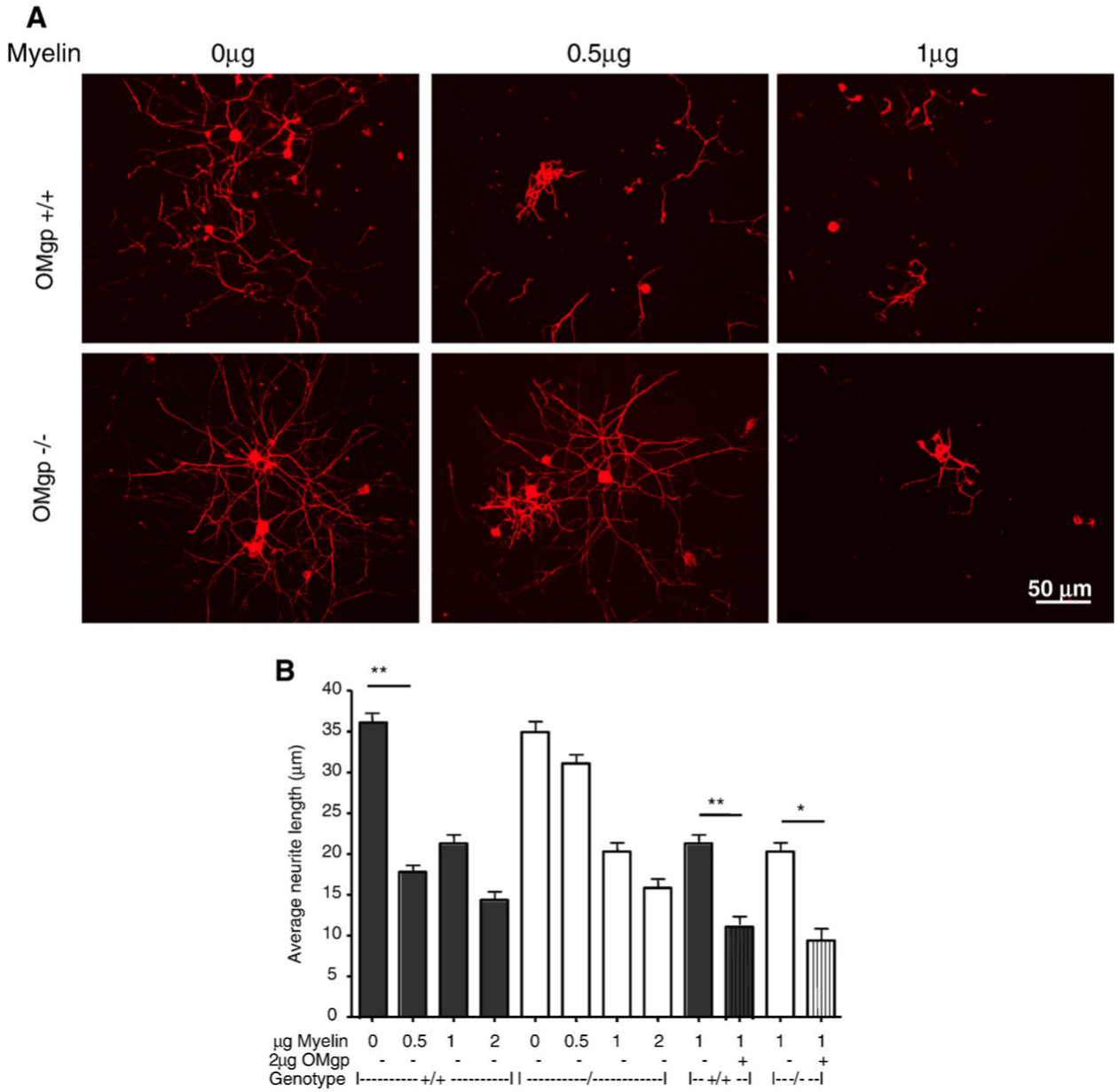

Fig. 8.

OMgp$^{-/-}$ myelin is less inhibitory. P6 rat DRG neurons were plated on myelin extracted from OMgp$^{-/-}$ or WT 129BL6 mice with or without AP-OMgp. Neurons were then cultured for 16 h prior to fixation and immunocytochemically labeled with anti-βIII tubulin antibody. (A) Examples of DRG neurons cultured in various concentrations of myelin substrates. (B) Quantification of the average neurite length of DRG neurons cultured on various substrates and concentrations. Data are presented as mean±SEM from 200 to 400 neurons analyzed by one-way ANOVA followed by Tukey's post-test comparing all unpaired data sets. * = P<0.05, ** = P<0.01.

Table 1

Average of BMS scores in the 129BL6 mice after dorsal-hemisection lesion

Days after injury	**1**	**3**	**7**	**14**	**21**	**28**	**35**	**42**
$OMgp^{+/+}$	3.73±0.74	4.36±0.67	4.64±0.28	4.91±0.25	5.18±0.35	5.27±0.33	5.32±0.36	5.50±0.40
$OMgp^{-/-}$	2.46±0.46	4.33±0.25	5.17±0.22	5.29±0.14	5.54±0.27	5.50±0.22	5.38±0.22	5.54±0.31

All data are represented as mean±SEM.

Table 2

Average of BMS subscores in the 129BL6 mice after dorsal-hemisection lesion

Days after injury	1	3	7	14	21	28	35	42
$OMgp^{+/+}$	2.18±0.73	3.00±0.89	3.00±0.75	3.09±0.74	2.64±0.98	3.64±0.79	3.55±0.87	4.36±0.93
$OMgp^{-/-}$	0.08±0.08	0.25±0.13	2.58±0.77	3.92±0.45	4.17±0.69	5.67±0.57	5.67±0.58	5.17±0.56

All data are represented as mean±SEM.

Table 3

Average of BMS scores in the BL6 mice after dorsal-hemisection lesion

Days after injury	1	3	7	14	21	28	35	42
OMgp$^{+/+}$	4.69±0.31	5.56±0.32	6.69±0.35	6.5±0.35	7.19±0.21	6.56±0.33	7.31±0.41	7.25±0.28
OMgp$^{-/-}$	3.67±0.73	4.89±0.52	5.89±0.42	5.78±0.33	6.11±0.48	6.28±0.38	6.39±0.42	6.11±0.48

All data are represented as mean±SEM.